ECM Machine Development and its Application in AISI 304 Machining

João M. V. de Sousa
joaomvsousa@tecnico.ulisboa.pt

Instituto Superior Técnico, Universidade de Lisboa, Portugal
June 2019

Abstract

Electrochemical machining (ECM) is a contactless non-conventional technology with the ability to process without tool wear any conductive material, regardless of its physical properties with an excellent commitment between dimensional accuracy and surface finish. Despite its advantages, it still urges for research of its field of application and operational conditions.

In this research, an ECM machine was developed that allowed the control of the manufacturing process operational parameters and subsequently the study of main operational parameters influence.

For the investigation, electrodes with 20 µm of diameter were used to machine AISI 304 specimens and the results demonstrate that the technology can be successfully used in machining slots and contours.

Key Words: machining, electrochemical micro machining, anodic dissolution, geometric tolerance, surface finishing.

1. Introduction

With the technological evolution comes up the necessity of ever more complex products with properties that surpass conventional barriers. Consequently to the miniaturization of products increases the demand of technologies capable of surpass the conventional machining capacities (Saxena et al. 2018).

However, with the miniaturization of products comes also instability, making it hard to rely on conventional machining technologies (Rosa 2008), therefore, in the last decades an effort has been made in the non-conventional technologies to coexist the complex requirements and the precise machining processes.

Non-conventional machining processes emerge to offer effective solutions to common issues like tool wear and heat generation at the tool and the workpiece interface (McGeough 1974). Among the non-conventional technologies, the electrochemical machining (ECM) stands out as an advantageous process without tool wear and surface stress, furthermore, it can machine complex shapes with smooth surfaces in conductive materials, regardless of their physical properties (Bhattacharyya et al. 2002).

The ECM technology is based on the anodic dissolution phenomenon and even though it has been pointed as a promising process there are a series of technical issues that difficult its implementation in a widely range of industries (Landolt et al. 2003).

When ECM is adapted to micromachining it is denominated as electrochemical micro machining (µECM), whereas the abovementioned advantages are even more appreciated, however, since the material removal phenomenon is based on electrochemistry, it has high sensitivity to process parameter variation, that is, each configuration of electrolytic solution and its material to be machined presents a particular behaviour when exposed to different electrical parameters, as well as, different tool geometries and flow through the gap (Davydov et al. 2004), which means that further research on those subjects, in order to better understand their influence on the process is required.

The main goal of this work was to contribute for a better understanding of the role played by some the process parameters from a technological point of view.

2. Experimental Development

Considering the major requirements for the development of the machining trials an experimental apparatus has been developed consisting in various subsystems assembled according to the objectives of this research.

2.1. Development of Experimental Apparatus

2.1.1. Machine Tool Structure

In order to overcome the corrosive environment to which the machine is subjected, the components are made of polymer, that is, PVC was used for the main structure and acrylic for the tool grip, likewise, the electrical connections to both electrodes pass through the structure interior to prevent them from being corroded as illustrated in Figure 1.

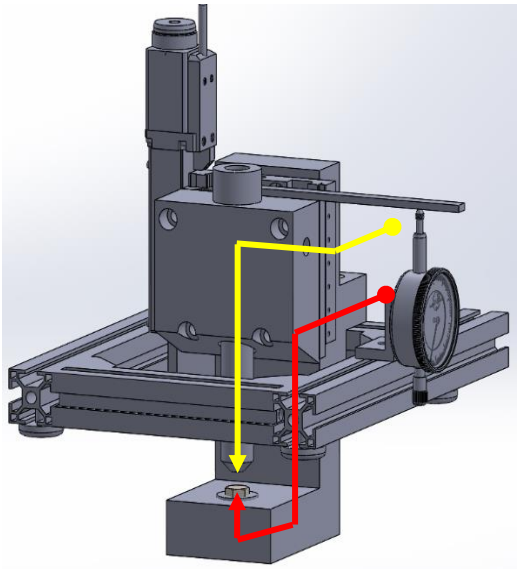

Figure 1: Illustration of electrical connections.

The main structure was integrated with a secondary structure made of aluminium that lays on the electrolyte tank and it is structurally adaptable to different types of tanks. The objective of this structure was to promote structural rigidity to the main structure as well as electrical insulation, using rubber feet.

The main structure can be divided in two parts: the static worktable where is the sample to be machined (anode) which is totally immersed inside the tank and the motorized part which permits the vertical translation of the tool, submerging it only when it is necessary. Note that, in this first version of the tool grip the electrolyte solution circulated inside the tool in order to help cleaning the machining zone. Also, a comparator clock was integrated in the structure to verify the relative distance between the electrodes.

All the design options considered a high repeatability of the trials, meaning the structure has to be tough enough to ensure consistence and practical enough to make the operators handling easier (Figure 2).

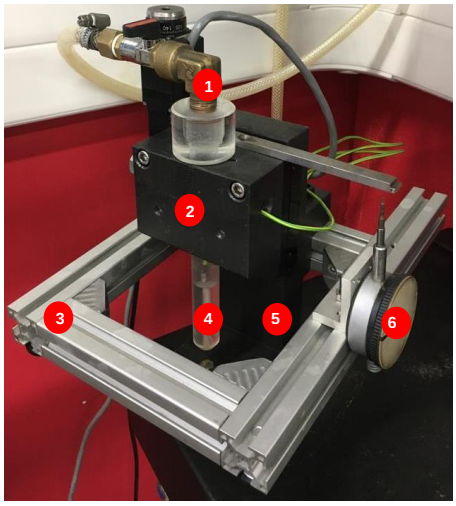

Figure 2: Machine tool elements: 1 – Electrolyte injection circuit; 2 – Mobile head; 3 – Secondary Structure; 4 – Tool grip; 5 – Fixed head; 6 – Comparator clock.

2.1.2. Electrolyte Circuit

The electrolyte circuit consists of a cylinder with solution pressurized using compressed air from the laboratory that forces the injection of electrolyte inside the tool and consequently its circulation on the machining zone, being also possible to regulate the output flow with a pressure regulator. The components of the electrolyte circuit were also made in polymer to prevent corrosion.

2.1.3. Servo mechanisms of motion

For the development of the trials, only vertical movement of the tool is needed. Thereby, a linear motor, *Standa* 8MT167-25LS, with high resolution, stability and speed, was attached to the mobile head.

Since this linear motor has a high movement resolution, because of its precision, it was extremely helpful whenever the gap between the electrodes was lower than 1mm.

2.1.4. Power Supply Circuit

Since studies previously developed have shown that pulsed power supply can reduce gap sizes, improving machining tolerances and also enables the recovery of the gap conditions during the pulse-off time, allowing improved dissolution efficiency (Rajurkar et al. 1993), the power supply was developed with only pulsed current conditions. The circuit developed is divided in three essential parts as demonstrated in Figure 3.

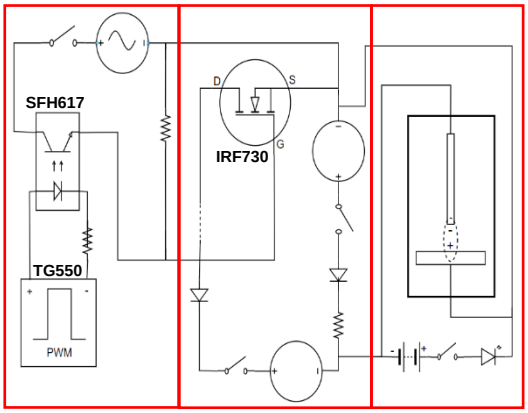

Figure 3: Design of electrical circuit.

At the left-hand side of the above figure it is represented the signal control section, in which a function generator, TTI TG550, allows the modulation of the digital signal, where it is possible to change parameter such as frequency, amplitude, pulse on time and pulse off time.

Between the signal control side and the mid parcel of the above figure, which is the power section, there is normally a galvanic isolator, to avoid disturbance of the high voltages/currents in the signal control, thereby, an optocoupler SFH617A was used.

Regarding the power section, the main component for the process to function is the Metal Oxide Semiconductor Field Effect (MOSFET) IRF730, which is a transistor that works like a switch and opens whenever it is applied a certain voltage to its terminals, hence letting current pass through.

At the right-hand side of the image are represented both electrodes as well as an LED that lights whenever the electrodes touch each other, thus giving the relative position of the tool relative to the workpiece.

The final detail of the circuit also represented at the right-hand side of the image is a *signal inverter*. Basically, in high frequency pulsed operations, the potential between electrodes does not really fall to zero (0V) during the pulse off time, however, with the *signal inverter*, the potential is forced to values near zero or even negative values, during the pulse-off time. In Figure 4 is shown the representative signal of the process.

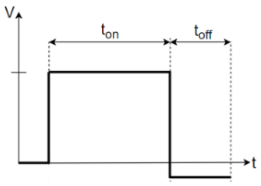

Figure 4: Electrical signature of the process.

In the end, after the design of the electrical circuit, it was simulated in a breadboard and afterwards developed in a real board as shown in Figure 5.

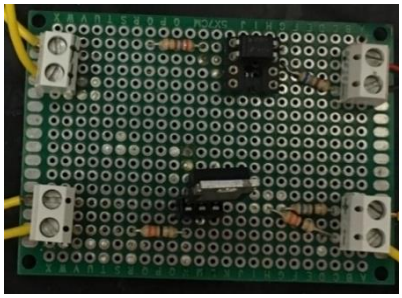

Figure 5: Experimental aparatus electrical circuit developed.

2.2. Tools

The tool with which the first experiments were developed is represented in Figure 6.

Figure 6: Tool used for the exploratory experiments.

This copper electrode has an exterior diameter of 1.1mm and an interior diameter of 0.3 mm in which the electrolyte solution circulates.

2.3. Experimental Apparatus

The full assembly of the various independent subsystems referred above is represented in Figure 7.

Figure 7: Final configuration of experimental apparatus.

2.4. Experimental planning

Considering the previously defined objectives for this research, an experimental planning was developed, and it was divided into two primordial parts: (i) exploratory analysis where a set of trials were developed to validate the structure integrity of the machine as well as the process functionality where parameters such as electrode roughness, electrolyte flushing, molar concentration, electrolyte temperature and even the introduction of an ultrasonic bath in the process were analysed; (ii) scientific analysis in order to study the geometric tolerances where frequency variation behaviour was evaluated to different molar concentrations of sulfuric acid, whilst for the surface roughness analysis the frequency was maintained constant as well as the current while changing the molar concentration. For this second stage an actual plan was developed represented in Table 1.

Table 1: Experimental planning.

Tool Material	Cooper
Sample Material	AISI 304
Tool Area [mm^2]	0.016
Electrolyte	H_2SO_4
Frequency (f) [kHz]	**5, 50, 500**
Concentration (M) [mol/L]	**0.1, 0.3, 0.5**
Current (A) [A]	0.6
Duty Cycle (d) [%]	40
Signal Inverter	On
Flushing	Off
Ultrasonic Bath	Off
Temperature (T) [ºC]	19
Depth [µm]	100
Feed (a) [µm]	15
Feed Rate [µm/min]	5

3. Results and Discussion

3.1. Exploratory Analysis

At this phase a verification analysis was necessary where parameters were randomly varied until an ideal range of operation parameters was obtained. Thereafter, some cavities were qualitatively analysed, being the frequency influence the first parameter analysed, as represented in Figure 8. The complementary analysis of these machined cavities shows the existence of shine dark material surfaces resulting from chemical reactions in the electrolyte deposited in electrode surface as shown in Figure 9.

a) b) c)

Figure 8: Obtained cavities for: (a) 50 kHz; (b) 100 kHz; (c) 150 kHz (M=0.15 mol H_2SO_4/L; V=6V; A=0.6A; d= 50%; T= 18.5ºC; a = 10µm; flushing on).

According to figure above, increasing the frequency, keeping other parameters constant, contributes to well-defined machined cavities.

During these first experiments, as it is possible to verify in the last figure, some irregularities were observed in the machined cavities, thereby, an explanation to this phenomenon was sought, starting with the electrode surface analysis before and after performing a trial, represented in Figure 9.

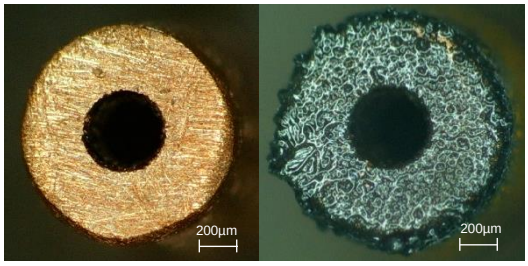

Figure 9: Tool front surface: before (left) and after (right) an experiment.

When machined products are deposited in the electrode surface during the experiment, as shown in the right-hand figure above, that creates a false geometry which introduces worse dimensional tolerances and surface finishing. Therefore, possible causes and solutions to this phenomenon were analysed.

3.1.1. Tool Surface Roughness

The surface roughness promotes the existence of micro geometries in the electrode surface that permits host of reaction products in the electrode surface. The Figure 10 show the influence of initial surface condition of the electrode in the obtained cavities. Qualitatively analysing, better results were obtained regarding the machine cavities with electrode polished with pastes. In Figure 11 is represented the electrode surface of the paste polished electrode after the experiment, where a significant reduction of machining muds in the surface is verified.

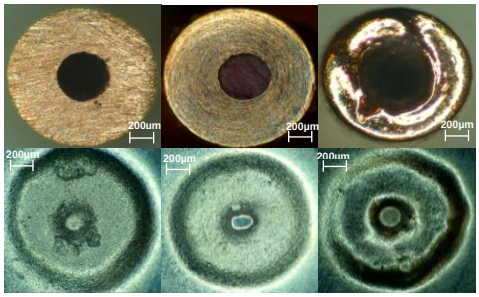

a) b) c)

Figure 10: Tool surface roughness analysis: (Top) Electrode surface rugosity obtained with: (a) water paper 150; (b) polishing pastes; (c) electrochemical polishing; and its respective machined cavities (f=150 kHz; M=0.15 mol H_2SO_4/L; V=6V; A=0.6A; d= 50%; T= 18.5ºC; a = 10µm; flushing on).

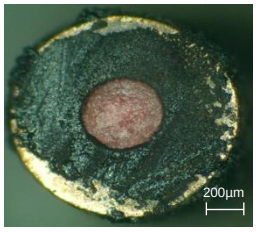

Figure 11: Rugosity analysis - Surface of the electrode after machining (polishing with pastes).

3.1.2. Electrolyte Flushing

The electrolyte flushing permits the renewal of the operation conditions in the electrodes interface. In the present investigation an electrode with 0.3 mm inner diameter was used to flush the electrolyte through the electrode gap. However, the reduced gap between electrodes strangle the electrolyte flow in the gap. This limitation could only be surpassed increasing the flow circulation pressure which would increase significantly the vibrations induced in the tool electrode and consequently on the workpiece electrode.

Some tests have been made to integrate a pump outside the machine forcing the circulation of electrolyte in machining zone, though unwanted vibrations were introduced in the electrode, so it would not be a viable option as well.

3.1.3. Ultrasonic Bath

To improve the cleansing mechanism of the process, a tank with ultrasonic cleaning *JARCOM PS-10A* was introduced, yet, an analyse of its advantages and disadvantages was extremely important. Naturally, the great advantage introduced is provide favourable flushing conditions in machining zone, while its disadvantage is the appearance of unexpected vibrations in the machining process.

In order to prevent the vibrations influence in the process, the secondary structure (aluminium) was separated from the tank, isolating both systems, being the electrolyte the only means of propagating vibrations. This analysis is presented in Figure 12.

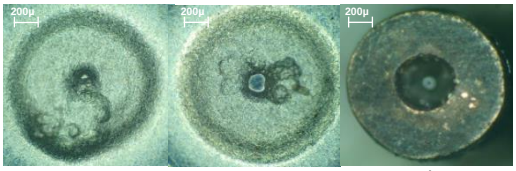

a) b) c)

Figure 12: Analysis on ultrasonic cleaning influence: (a) Non-isolated; (b) Isolated; (c) Electrode (f=150kHz; M=0.15 mol de H_2SO_4/L; V=6V; A=0.6A; d=50%; T=18.5ºC; a=10µm; flushing off).

3.1.4. Molar Concentration

The molar concentration is related with the ion concentration in the process and with capacity of the process to remove metallic ions of the specimen. On the other side, higher acid concentration promotes secondary chemical reactions which dissolve some reaction products in the acid electrolyte, decreasing the adherence of those products in the electrode surface. This hypothesis is supported with the results shown in Figure 13 which represents the increase of sulfuric acid molar concentration to 0.3 mol per litter of distilled water.

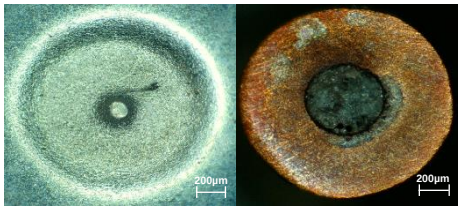

Figure 13: Machined cavity and electrode after machining with molar concentration of 0.3 mol de H_2SO_4/L (f=150kHz; V=6V; A=0.6A; d=50%; T=18.5ºC; a=10µm; flushing off; ultrasonics on).

3.1.5. Electrolyte Temperature

The ultrasonic cleaner integration gave the opportunity to control the temperature of the electrolyte, thereby a quick analysis of its influence was developed, represented in Figure 14. There is no significant improvement in the results obtained regarding the reaction products deposition in electrode surface.

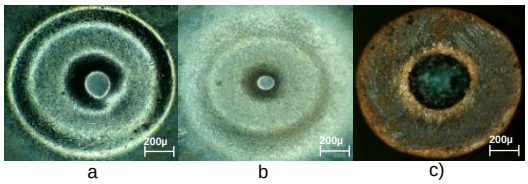

Figure 14: Machined cavities and respective electrode (c) with: (a) 35ºC; (b) 50ºC (M=0.3 mol de H_2SO_4/L; f=150kHz; V= 6V; A=0.6A; d=50%; a=10µm; ultrasonics off; flushing off).

3.2. Application in the wire machining of AISI 304

Considering the exploratory analysis developed before, some modifications have been made to the apparatus. As previously mentioned, this technology is improved when adapted to micro machining. Thereby, a new tool with 20 µm copper wire was adapted to the machine with intention to reduce the scale, whereas a new support for the tool was also developed, as well as, a new support for the specimens. To develop these components, represented in Figure 15 and Figure 16, it was necessary to use, turning, milling and even electrical discharging machining (EDM), as it is possible to see at right-hand side of Figure 16.

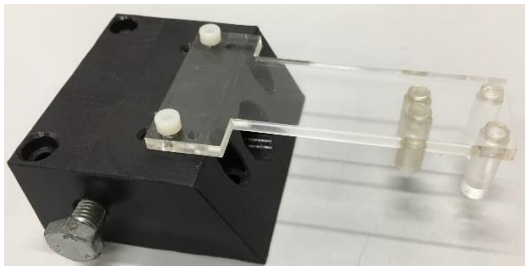

Figure 15: Fixation mechanism for 20 µm tool.

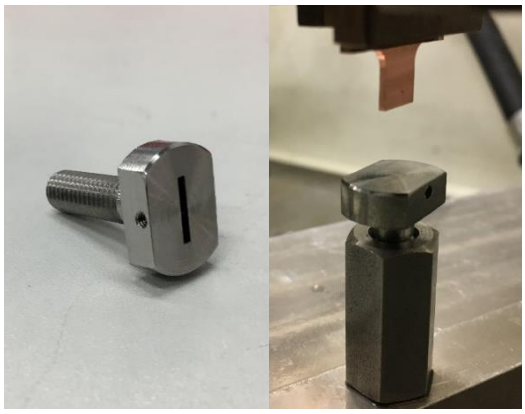

Figure 16: Specimens support (Left) developed with EDM (Right).

Note that, the technology was optimized with scale reduction, as well as, with the polished surface that the copper wire had.

With these components, conditions were reunited to development of the scientific analysis, being the machining zone with the configuration presented in Figure 17.

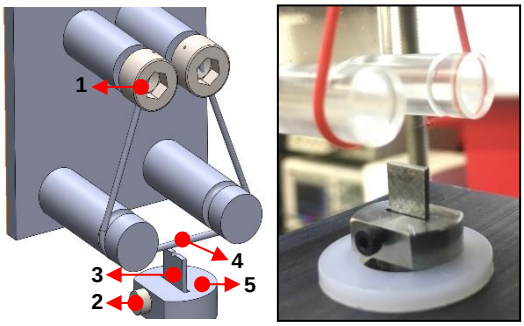

Figure 17: New tool configuration (1 - Tighteners; 2 - Specimen holding; 3 - Specimen; 4 - Wire (tool); 5 - Specimen housing).

Before each test the tool was replaced, and the comparator clock was zeroed. The experiments started with 20 µm gap between electrodes and lasted approximately 25 minutes, after which the specimen was removed and analysed in an optical microscope, where images were obtained, as shown in Figure 18 for further analysis.

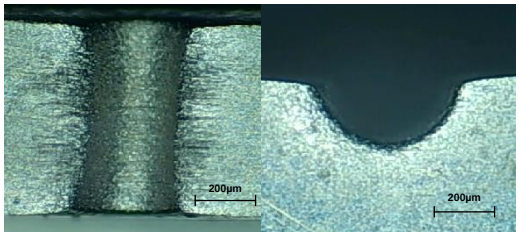

Figure 18: Top and side view of µECM machined surface with 20 µm tool.

3.2.1. Machined profiles

The variation of main parameter of the process can deeply affect the geometric accuracy of a µECM operation as the Figure 19, 20 and 21 demonstrate, where machined profiles behaviour is shown for frequency variation (5, 50, 500 kHz) with different molar concentrations (0.1, 0.3, 0.5 mol H_2SO_4/L) of sulfuric acid.

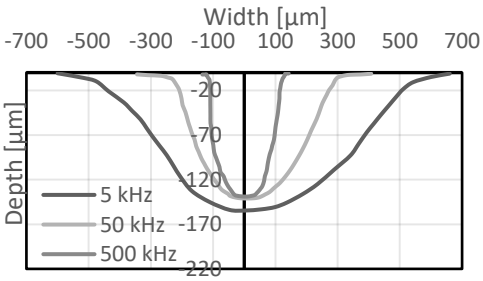

Figure 19: Evolution of machined profiles (µm) as function of frequency (5, 50, 500 kHz) for 0.1 mol de H_2SO_4/L (A=0.3A; d=40%; T= 19ºC; inverter on; ultrasonics off; flushing off; a=5 µm/min; gap=20 µm).

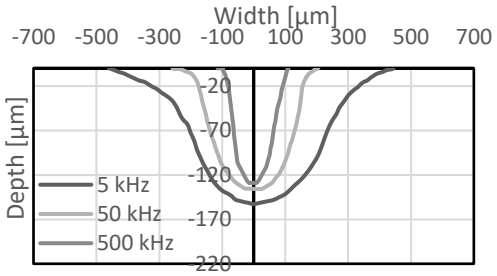

Figure 20: Evolution of machined profiles (µm) as function of frequency (5, 50, 500 kHz) for 0.3 mol de H_2SO_4/L (A=0.3A; d=40%; T= 19ºC; inverter on; ultrasonics off; flushing off; a=5 µm/min; gap=20 µm).

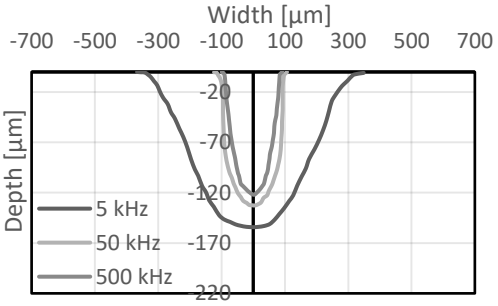

Figure 21: Evolution of machined profiles (µm) as function of frequency (5, 50, 500 kHz) for 0.5 mol de H_2SO_4/L (A=0.3A; d=40%; T= 19ºC; inverter on; ultrasonics off; flushing off; a=5 µm/min; gap=20 µm).

3.2.2. Geometric Tolerance

Regarding geometric tolerance analysis, the machined profiles where evaluated and outlined in Figure 23, 23 and 24. As it is possible to observe, the frontal gap, lateral gap and entrance fillet tend to decrease as frequency increases. In other words, increasing the frequency increases geometric accuracy.

Due to current increasing dispersion while deepening the machining profile the side gap is normally bigger than frontal gap, also observed in the figures below.

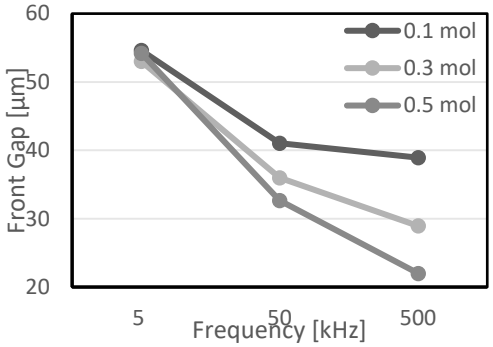

Figure 22: Front gap (µm) evolution as function of frequency (5, 50, 500 kHz) for different molar concentrations (0.1, 0.3 e 0.5 mol H_2SO_4/L)(A=0.3A; d=40%; T= 19ºC; inverter on; ultrasonics off; flushing off; a=5 µm/min; gap=20 µm).

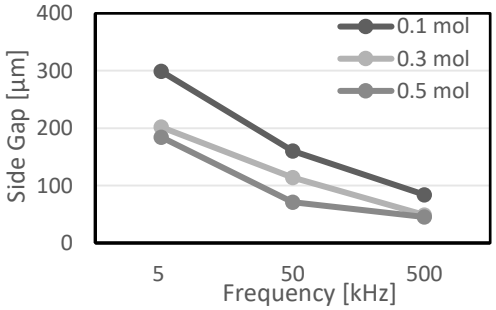

Figure 23: Side gap (µm) evolution as function of frequency (5, 50, 500 kHz) for different molar concentrations (0.1, 0.3 e 0.5 mol H_2SO_4/L)(A=0.3A; d=40%; T= 19ºC; inverter on; ultrasonics off; flushing off; a=5 µm/min; gap=20 µm).

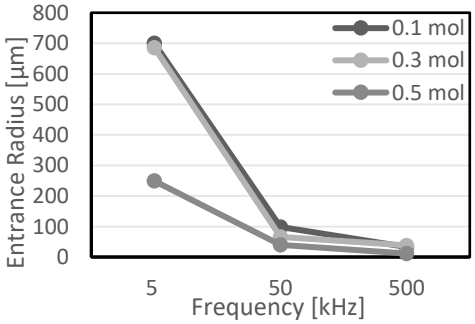

Figure 24: Entrance radius (µm) evolution as function of frequency (5, 50, 500 kHz) for different molar concentrations (0.1, 0.3 e 0.5 mol H_2SO_4/L)(A=0.3A; d=40%; T= 19ºC; inverter on; ultrasonics off; flushing off; a=5 µm/min; gap=20 µm).

3.2.3. Surface Finishing

The surface finishing study of machined surfaces, involved the variation of molar concentration, maintaining current parameter constant and consequently material removal rate (MRR) also constant, thereby, with these conditions similar geometries were obtained which permitted the correct comparison between them.

When it comes to surface finishing, a qualitative analysis was developed, due to the difficulty to measure roughness on the interior of a 200 µm machined groove. The analysis is resumed in Figure 25.

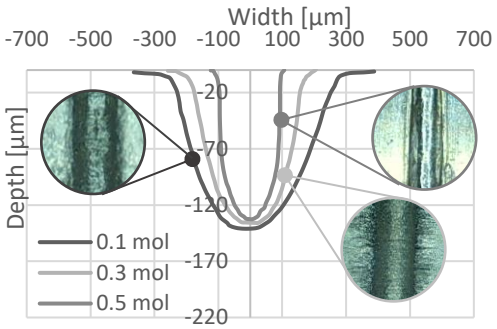

Figure 25: Machined profile (µm) evolution with 50 kHz frequency for different molar concentrations (0.1, 0.3 e 0.5 mol H_2SO_4/L) and respective surface quality analysis (A=0.3A; DC=40%; T= 19ºC; inverter on; ultrasonics off; flushing off; a=5 µm/min; gap=20 µm).

Hence, analysing the above figure, while molar concentration increases the surface roughness tends to improve.

6. Conclusion

The experimental apparatus developed proved to be reliable, functional, as it stood up to all the experiments developed while being handy to use. The experimental research on AISI 304 µECM using copper tool, with an H_2SO_4 electrolyte where variation in some primordial parameters (frequency, molar concentration) lead to a better understanding of the process behaviour. Considering the main objectives stipulated and the application of the technology to industry, promising data was acquired regarding geometric tolerance and surface finish, varying only two essential process parameters. By properly selecting the machining conditions, more predictable µECM results can be achieved, reiterating it as a promising technology in this field.

References

Bhattacharyya, B., S. Mitra, e A.K. Boro. 2002. «Electrochemical micro-machining : new possibilities for micro-manufacturing». *Robotics and Computer Integrated Manufacturing*, n. 18: 283–89.

Davydov, A. D., V. M. Volgin, e V. V. Lyubimov. 2004. «Electrochemical machining of metals: Fundamentals of electrochemical shaping». *Russian Journal of Electrochemistry* 40 (12): 1230–65.

Landolt, D., P. F. Chauvy, e O. Zinger. 2003. «Electrochemical micromachining, polishing and surface structuring of metals: Fundamental aspects and new developments». *Electrochimica Acta* 48 (20–22): 3185–3201.

McGeough, J.A. 1974. *Advanced Methods of Machining*. London: Springer Netherlands.

Rajurkar, K.P., Jerzy Kozak, B. Wei, e J.A. Mcgeough. 1993. «tudy of Pulse Electrochemical Machining Characteristics». *CIRP Annals - Manufacturing Technology* 42 (1): 231–34.

Rosa, Pedro. 2008. «Processos Subtractivos». *Manual de Micromanufactura*.

Saxena, Krishna Kumar, Jun Qian, e Dominiek Reynaerts. 2018. «A review on process capabilities of electrochemical micromachining and its hybrid variants». *International Journal of Machine Tools and Manufacture* 127 (January): 28–56.